NDT&E International 42 (2009) 308–315

Contents lists available at ScienceDirect

NDT&E International

journal homepage: www.elsevier.com/locate/ndteint

Magnetic image detection of the stainless-steel welding part inside a multi-layered tube structure

Takayuki Hayashi [a,b,*], Yoshihiko Kawasaki [a], Hironobu Yamada [a], Toshihiko Kiwa [a], Masaji Tamazumi [c], Keiji Tsukada [a]

[a] *Graduate School of Natural Science and Technology, Okayama University, 3-1-1 Tsushima-naka, Okayama 700-8530, Japan*
[b] *Pulstec Industrial Co. Ltd., 7000-35 Techno-land, Hosoe, Kita-ku, Hamamatsu, Shizuoka 431-1304, Japan*
[c] *Uno Kogyo Co. Ltd., 6-1, Tamahara 3-chome, Tamano, Okayama 700-0014, Japan*

ARTICLE INFO

Article history:
Received 8 August 2008
Received in revised form
4 December 2008
Accepted 8 December 2008
Available online 24 December 2008

Keywords:
Non-destructive evaluation
Magnetoresistive sensor
Stainless-steel weld
Low-frequency magnetic field

ABSTRACT

The stainless-steel welding part inside a multi-layered tube was successfully detected using low-frequency magnetic imaging. The magnetic images were obtained by the developed measurement system, consisting of an exposure coil, magnetoresistive (MR) sensor, lock-in amplifier, x–y stage, revolving stage with a horizontal level stage and personal computer. To expose the magnetic field to a wide area of the stainless-steel sample, the radius of the exposure coil was made comparable to the sample size. The MR sensor measured the vector components of the magnetic field generated from the sample within the range of low frequencies between 50 Hz and 1 kHz. A cylindrical stainless-steel sample was fabricated as a tube by rolling a stainless-steel sheet and welding each edge using arc welding with argon as shielding gas. The normal components (B_z) and tangential components (B_x and B_y) to the sample surface were measured by scanning the MR sensor on the sample surface and the magnetic characteristics of each of the component images were documented. As a result, the difference in permeability between the weld area and the base material was successfully visualized as magnetic images.

1. Introduction

Welding is a technique used in many industries, including nuclear power stations, aerospace, automobiles, shipbuilding, etc. With the recent increases in weld quality control requirements, the non-destructive evaluation (NDE) of welding has been increasingly required for quality control or maintenance management purposes. Various types of NDE techniques for welds, such as ultrasonic inspection [1,2], X-ray inspection [3] and magnetic inspection [4], are asked for by standards. The eddy current NDE, which is a common form of magnetic inspection, is a useful technique for detecting defects, flaws, or discontinuities in electrically conductive materials. The principle of eddy current NDE is based on Faraday's law. When a magnetic field, which is generated by transmitting an AC current through a coil, is generated and penetrates into a conductive material, eddy currents are induced in the material and decrease the magnetic field. Subsequently, the eddy currents generate a secondary magnetic field, the distribution of which is associated with that of the eddy currents. Therefore, when the eddy current distribution is changed due to any flaw in the sample, the generated secondary magnetic field is also changed, and the eddy current NDE technique detects the change in the generated secondary magnetic field, which is sensed by a receiving coil or field-sensitive sensors measuring the superposition of the primary and secondary fields or by measuring the impedance of the receiving coil. To detect deeper flaws in the sample, eddy current NDE requires operation with a low-frequency magnetic field, since the larger the skin depth, the lower the frequency of the magnetic field is required. With this in mind, magnetic sensors, such as magnetoresistive (MR) sensors [5,6] or superconducting quantum interference devices (SQUID) [7,8], which can operate at low frequencies, have been studied and used to detect deeper flaws.

In addition, magnetic imaging techniques have been developed for the eddy current NDE. We developed a low-frequency magnetic field imaging system in order to obtain the two-dimensional image of magnetic field fluctuations by analyzing three-dimensional magnetic field components [9]. In the case of the nonmagnetic Al samples, the images of magnetic field fluctuations were measured by direct eddy current imaging. Moreover, in the case of the ferromagnetic iron samples, images of the magnetic field fluctuations were obtained by both local

---

[*] Corresponding author at: Graduate School of Natural Science and Technology, Okayama University, 3-1-1 Tsushima-naka, Okayama 700-8530, Japan.
Tel./fax: +81 086 251 8129.
E-mail address: t-hayashi@sense.elec.okayama-u.ac.jp (T. Hayashi).

0963-8695/$ - see front matter © 2008 Elsevier Ltd. All rights reserved.
doi:10.1016/j.ndteint.2008.12.006

magnetization of the sample and direct eddy current imaging. Further applications including the detection of cracks in samples with bulk or multi-layered structures by direct eddy current imaging [10], and detection of a discontinuity in Al samples with bulk or multi-layered structures by line scanning of the normal magnetic field component [11] were reported. By using the system to measure normal components, we detected the change in the magnetic properties of the stainless-steel welding part, welded under argon shielding gas condition [12].

In this paper, we applied the low-frequency magnetic field imaging methods to visualize the magnetic response of the stainless-steel weld area. A comparison of the normal and tangential magnetic field components have been indicated that in the magnetic response the effect of the eddy currents and the focused magnetic flux based on high-permeability values can be distinguished. We proceed with investigations of the magnetic imaging method not only to visualize the weld area on the surface, but also to visualize the weld area inside the multi-layered tube.

2. Measuring system

A novel experimental set-up for detecting the three-dimensional distribution of the magnetic field was developed. Fig. 1 shows a schematic diagram of the magnetic imaging system, which consists of an exposure coil, an MR sensor, a lock-in amplifier, an *x*–*y* stage, a revolving stage with a horizontal level stage and a personal computer. The stainless-steel sample was exposed to a primary magnetic field, generated by the induction coil, while the MR sensor measured that was generated by the sample. The normal sensitive axis of the MR sensor and the normal axis of the induction coil were set along the *Z*-axis. The type of MR sensor used was an anisotropic magnetoresistive (AMR) sensor (Honeywell, HMC2003). The MR sensor measured the three magnetic field components, which include the normal (*z*) and tangential (*x* and *y*) components of the sample surface.

The diameter of the induction coil was 0.8 m with 40 turns, and the distance between the induction coil and the MR sensor was maintained at 0.5 m. The induction coil was driven by sinusoidal currents. The frequencies of the driven currents were 50 Hz to 1 kHz, with peak-to-peak amplitude of 1 A. The amplitude of the induced magnetic field was 4.0 μT at the sample surface measured along the induction coil center axis.

The MR sensor output signals were detected at the frequency of the electric current in the induction coil. The signals were separated into the magnetic field strength amplitude and the phase shift to the induction magnetic field, using a lock-in amplifier.

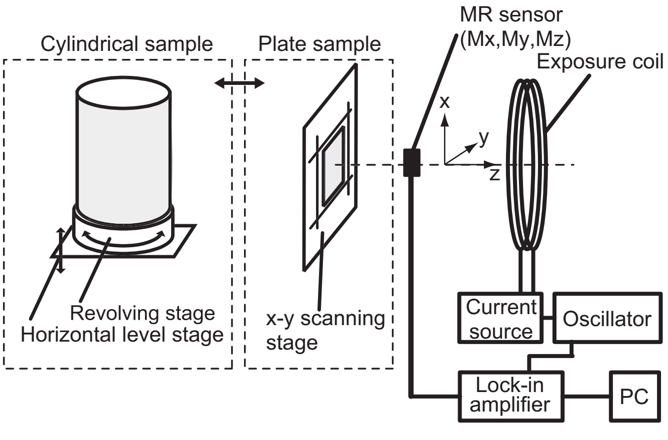

Fig. 1. Schematic diagram of the magnetic property imaging system.

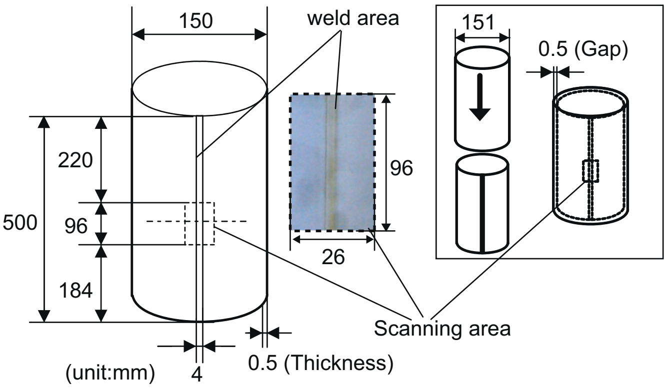

Fig. 2. Schematic diagram of the cylindrical stainless-steel sample and one part of the sample photograph. The inset is the schematic diagram of the multi-layered sample.

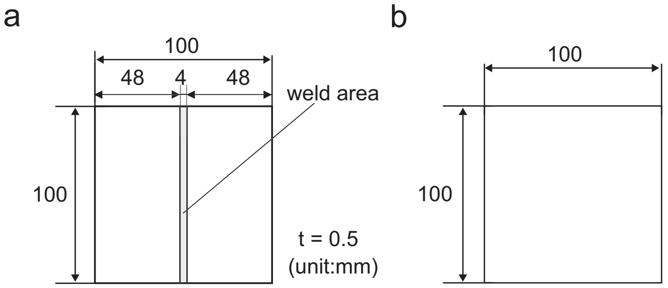

Fig. 3. Schematic diagram of the stainless-steel square sample: (a) with weld and (b) without weld.

The cylindrical stainless-steel sample and a square flat plate of stainless-steel were produced. The cylindrical stainless-steel sample was made by rolling a stainless-steel sheet (SUS 304) and by welding lengthwise using arc welding with argon as shielding gas (Fig. 2). The square flat plate sample made of stainless-steel was produced by welding two pieces of a stainless-steel sheet (Fig. 3). The thickness of the stainless-steel sheet was 0.5 mm. The welds were made with a tungsten electrode (TIG308) and the width of the weld area was 4 mm. The diameter of the cylindrical sample was 150 mm, and the height was 500 mm. The multi-layered tube was produced by having the inner tube with a slightly smaller diameter pushed into the outer tube. The weld area of the outer tube was set in the 180° position in the opposite direction of the weld area of the inner tube. The diameter of the outer tube was 151 mm, and the gap between the inner and outer samples was 0.5 mm. The size of the square flat plate sample of stainless-steel was 10 cm on one side, and the weld area was located on the centerline of the square. To clarify the effect of the welding part on the magnetic imaging, a square flat plate sample of stainless-steel, but without a weld, was also produced for reference.

The scanning area of the cylindrical stainless-steel sample surface was 96 mm in height and 26 mm in width, while the vertical center of the scanning area included the 4 mm width of the weld area. For stepwise scanning on the cylindrical stainless-steel sample surface, the pitch size was selected at about 10 mm in height, and 1.3 mm in width, respectively. The distance between the sensor and the sample surface was maintained at 3 mm during the scanning process. To scan the sample surface, the cylindrical stainless-steel sample was set on a horizontally rotating platform with a facility to adjust the height. The square flat plate stainless-steel sample was set on the *X*–*Y* scanning device (Fig. 1).